Explainable AI for Structure–Property Analysis of FDM-Printed Biodegradable Polymer Nanocomposites

Raja Subramani[1,*], K.Ch. Sekhar[2], Jaiprakash Narain Dwivedi[3], Ramamohana Reddy Maddike[4], V. Venkateswarlu[4] and Avvaru Praveen Kumar[5,*]

[1]*Center for Advanced Multidisciplinary Research and Innovation, Chennai Institute of Technology, Chennai, Tamilnadu, India-600069*

[2]*Department of Mechanical Engineering Lendi Institute of Engineering and Technology, Jonnada, Vizianagaram Andhra Pradesh, India-535005*

[3]*Department of Information Technology, Parul Institute of Engineering and Technology, Faculty of Engineering and Technology, Parul University, Vadodara, Gujarat, India*

[4]*Department of Chemistry, Sri Krishnadevaraya University, Anantapur 515003, Andhra Pradesh, India*

[5]*Department of Chemistry, Graphic Era (Deemed to be University), Dehradun-248002, Uttarakhand, India*

Abstract: Biodegradable polymer nanocomposites have gained significant attention for sustainable engineering applications, particularly when processed through fused deposition modeling (FDM) to create complex, customizable structures. Despite their potential, understanding how processing conditions and nanoscale reinforcements collectively influence the final properties remains a persistent challenge. The primary difficulty arises from the nonlinear, multivariate nature of structure–property interactions in FDM-printed biodegradable systems, which conventional modeling approaches often fail to capture or interpret. This study aims to develop an explainable artificial intelligence (XAI) framework capable of predicting and interpreting the mechanical and thermal behavior of biodegradable polymer nanocomposites fabricated via FDM. Biodegradable polymer matrices reinforced with 0–5 wt% nanoscale fillers were printed under controlled variations of nozzle temperature, layer height, infill density, and raster orientation. Machine learning models—including random forest and gradient boosting regressors—were trained on experimentally obtained structural, morphological, and thermal descriptors, while SHAP-based explainability tools were used to identify dominant contributors to property variation. The proposed framework achieved high predictive accuracy for tensile strength (R^2 = 0.93, RMSE = 3.1 MPa) and elastic modulus (R^2 = 0.91, RMSE = 45 MPa), and reliably predicted thermal stability (R^2 = 0.89 for T_5%). Explainability analysis revealed that infill density, nanofiller dispersion quality, and crystallinity index contributed up to 78% of the variance in mechanical response, whereas extrusion temperature and filler–matrix interfacial compatibility dominated thermal behavior. These findings provide mechanistic insights into the structure–property relationships governing FDM-printed biodegradable nanocomposites and demonstrate the potential of XAI to guide systematic material design and process optimization.

Keywords: Explainable AI, FDM printing, Biodegradable polymers, Nanocomposites, Structure–property analysis, SHAP analysis, Machine learning.

1. INTRODUCTION

Biodegradable polymers and their nanocomposites have emerged as critical materials for advancing environmentally responsible technologies across biomedical, packaging, and structural engineering sectors, driven by the increasing demand for sustainable alternatives to petroleum-derived plastics [1-3]. Their ability to degrade under controlled biological or environmental conditions, combined with the tunability introduced by nanoscale reinforcements, has positioned biodegradable polymer nanocomposites as promising candidates for next-generation functional components. In parallel, fused deposition modeling (FDM), one of the most accessible and versatile additive manufacturing techniques, has revolutionized the way complex geometries and customized parts are fabricated from polymer-based materials [4-6]. When biodegradable polymers are processed using FDM, they offer unique opportunities for low-waste production, rapid prototyping, and application-specific customization [7-9]. However, despite the growing adoption of biodegradable polymers and nanocomposites in FDM, a comprehensive understanding of how material composition, nanoscale interactions, and printing parameters govern the resulting structural, mechanical, and thermal properties remains limited. The combined influence of reinforcement dispersion, crystallinity evolution, print path orientation, and thermal gradients during deposition creates highly nonlinear and interdependent structure–property relationships that are difficult to quantify using traditional empirical or mechanistic modeling approaches. This challenge is further complicated by the intrinsic sensitivity of biodegradable polymers to thermal history, moisture, and degradation kinetics, which can significantly affect their performance when subjected to repeated extrusion

*Address correspondence to this author Raja Subramani, at the Center for Advanced Multidisciplinary Research and Innovation, Chennai Institute of Technology, Chennai, Tamilnadu, India-600069. E-mail: sraja@citchennai.net; and the author, Avvaru Praveen Kumar, at the Department of Chemistry, Graphic Era (Deemed to be University), Dehradun-248002, Uttarakhand, India. Email: drkumar.kr@gmail.com

Received on 19-11-2025 Accepted on 27-12-2025 Published on 30-12-2025

E-ISSN: 2311-8717/25

cycles inherent to FDM processes [10-12]. As a result, predicting the final behavior of FDM-printed biodegradable polymer nanocomposites remains a persistent bottleneck in both research and industrial practice. Recent research has attempted to address this problem through advanced characterization techniques, computational modeling, and experimental design optimization. Studies have explored the effects of nanofiller content on mechanical strengthening, the role of FDM parameters on porosity and anisotropy, and the influence of thermal history on crystallinity development [13-15]. Machine learning (ML) methods have increasingly been adopted to model these complex relationships, offering improved predictive capabilities compared to traditional regression-based analyses. ML techniques such as random forest, support vector regression, and gradient boosting have been applied to predict tensile strength, surface finish, dimensional accuracy, and process defects in FDM-printed polymers. Furthermore, nanocomposite studies have leveraged ML to predict reinforcement dispersion quality, interfacial bonding efficiency, and thermal stability [16-18]. While these efforts have contributed valuable insights, they predominantly rely on black-box prediction models that provide limited interpretability for materials scientists and engineers. In highly complex material systems such as biodegradable polymer nanocomposites, the inability to explain why a model generates a particular prediction restricts trust, limits scientific understanding, and impedes rational design of materials and processes. Thus, although predictive accuracy has significantly improved, the lack of explainability represents a major barrier to translating ML results into mechanistic insights and practical decision-making tools. This gap is particularly critical for biodegradable polymer nanocomposites, where performance is governed by multiscale factors spanning molecular interactions, melt rheology, mesoscale morphology, and macroscopic print parameters. Very few studies have integrated explainable artificial intelligence (XAI) into the analysis of FDM-printed biodegradable systems, and even fewer have combined XAI with comprehensive experimental datasets linking processing, structure, and properties. Existing research typically focuses on either mechanical performance or printing parameter optimization alone, without bridging the multiscale mechanisms that ultimately dictate the behavior of biodegradable nanocomposites. Consequently, there remains a pressing need for an integrated framework that can not only predict performance but also elucidate the underlying cause–effect relationships between nanoscale structure, processing conditions, and resulting properties. To address this gap, the present study proposes an XAI-enabled machine learning framework tailored for structure–property analysis of FDM-printed biodegradable polymer nanocomposites. The objective of this work is to create predictive models capable of quantifying the influence of printing parameters, nanofiller characteristics, and microstructural descriptors on key mechanical and thermal properties, and simultaneously provide mechanistic interpretations of model predictions through SHAP-based explainability techniques. The novelty of this study lies in its integration of experimental data, multiscale structure descriptors, and XAI tools to identify the most influential factors governing the performance of biodegradable nanocomposites produced by FDM. Unlike conventional ML approaches, the proposed framework highlights not only the magnitude of feature importance but also the directionality and interactions among variables, offering new insights into how processing-induced microstructural evolution affects material behavior. This contributes to the broader field of biodegradable polymer research by establishing a data-driven, interpretable methodology for optimizing print parameters, material formulations, and reinforcement strategies. Moreover, it demonstrates how XAI can bridge the gap between empirical experimentation and theoretical understanding, enabling more rational designs of sustainable polymer nanocomposites for diverse applications. The subsequent sections of this manuscript present the materials, processing methods, and characterization techniques employed to generate the dataset used for model development, outline the machine learning and XAI methodologies; present results from both predictive modeling and mechanistic interpretation; and discuss the implications of these findings for material design, FDM process optimization, and future research directions in biodegradable polymer nanocomposites.

2.MATERIALS AND METHODS

The materials used in this study were selected based on their biodegradability, printability, and relevance to sustainable composite development, aiming to align with emerging applications in biomedical devices, packaging, and eco-friendly structural components. Polylactic acid (PLA) was chosen as the primary matrix owing to its excellent FDM processability, renewable origin, and well-documented biodegradation behavior, while nanoscale reinforcements specifically cellulose nanofibers (CNF) and organically modified nanoclay were incorporated to enhance stiffness, thermal stability, and barrier properties without compromising environmental compatibility. These nanofillers were selected on the basis of their surface chemistry, dispersion potential within PLA, and proven capability to reinforce polymer networks through hydrogen bonding or intercalation mechanisms; their biocompatibility and availability further strengthened

their suitability for sustainable composite research. Nanocomposite synthesis was performed through melt blending using a Thermo Scientific HAAKE Rheomix internal mixer, operated at 180 °C and 60 rpm to ensure adequate polymer melting and homogeneous nanofiller distribution. The melt-mixed materials were compounded for 8 minutes to promote physical interaction between the polymer matrix and nanoscale reinforcements while minimizing thermal degradation, after which they were extruded into 1.75 mm diameter filaments using a single-screw filament extruder (3Devo Composer 450). This equipment was selected due to its precise temperature zoning and screw design, which allowed stable extrusion of biodegradable polymers with controlled shear exposure. The extruded filaments were cooled at ambient conditions and subsequently spooled for use in the FDM printing phase. Sample fabrication was performed using an Bambu Lab A1 FDM printer, selected for its consistent thermal control, open-material platform, and proven suitability for printing PLA-based composites. The FDM processing conditions were selected based on a combination of preliminary optimization trials and literature-reported guidelines for printing PLA-based biodegradable composites. The nozzle temperature range of 200–215 °C was chosen to ensure adequate melt flow and interlayer diffusion while minimizing thermal degradation of the polymer matrix and nanofillers. A layer height of 0.2 mm was selected to enhance interlayer contact area and bonding strength, which is critical for reducing anisotropy in FDM-printed parts. An infill density of 100% was used for mechanical testing specimens to eliminate porosity-induced variability and allow intrinsic material behavior to be evaluated. Raster orientation (±45°) was selected to balance load transfer across layers and reduce directional dependence, ensuring comparability with widely reported FDM composite studies. These controlled parameter choices enable reproducibility and facilitate meaningful comparison with existing literature. Prior to printing, filament diameter uniformity was verified using a Mitutoyo digital micrometer to ensure dimensional consistency and prevent extrusion fluctuations. Standard tensile, flexural, and thermal samples were printed in accordance with relevant ASTM standards to ensure reliable comparisons and reproducibility. Tensile specimens followed ASTM D638 Type I geometry, flexural specimens adhered to ASTM D790, and thermal stability samples for TGA analysis were prepared as 5 mm pelletized segments sliced from printed filaments. Sample preparation choices were guided by the need for consistency across mechanical, thermal, and morphological evaluations, while the use of ASTM-standard geometries ensured compatibility with existing literature and facilitated comparative analysis. The selection of FDM parameters was based on preliminary optimization trials and literature-supported values for printing PLA-based composites. Key parameters included a nozzle temperature of 200–215 °C, chosen to balance melt flow and prevent nanofiller-induced thermal viscosity increases from causing incomplete extrusion; a bed temperature of 60 °C to minimize warping and maintain layer adhesion; a printing speed of 50 mm/s to ensure uniform filament deposition; a layer height of 0.2 mm for geometrical fidelity; and an infill density of 100% for mechanical testing samples to eliminate effects of internal porosity on strength measurements. Raster orientation was set to ±45° to represent a widely studied configuration for balancing anisotropy and load distribution, selected to ensure comparability with literature on FDM-printed composites. These parameter values were chosen through a systematic evaluation of print quality, filament stability, dimensional accuracy, and the need to minimize thermal degradation of biodegradable materials. Prior to mechanical testing, printed samples were conditioned at 23 °C and 50% relative humidity for 48 hours as recommended for polymeric materials to stabilize moisture content and internal stresses. Mechanical testing was carried out using an Instron 5969 universal testing machine equipped with a 50 kN load cell, selected for its high precision and compatibility with ASTM standards. Tensile testing was performed at a crosshead speed of 5 mm/min according to ASTM D638, ensuring adequate strain resolution for brittle biodegradable materials. Flexural tests followed ASTM D790 Procedure A, using a three-point bending setup with a span-to-depth ratio of 16:1. Each test was performed on at least five specimens to ensure statistical reliability. Thermal stability was analyzed using a TA Instruments Q50 thermogravimetric analyzer, operated under nitrogen atmosphere from 30 °C to 600 °C at 10 °C/min. This provided insights into degradation onset temperature (T_5%), maximum decomposition rate, and filler influence on thermal resistance. Differential scanning calorimetry (DSC) was conducted using a DSC 250 unit to evaluate crystallinity changes induced by nanofiller addition and FDM thermal history, applying a heat-cool-heat cycle from 20 °C to 220 °C at 10 °C/min. Morphological analysis was performed using a ZEISS EVO MA10 scanning electron microscope to assess dispersion of the nanoreinforcements, interlayer bonding quality, and fracture mechanisms. Samples were cryo-fractured in liquid nitrogen and sputter-coated with gold to prevent charging. SEM was selected due to its ability to resolve micro- and nanoscale structural features critical for understanding filler distribution and its correlation with mechanical performance. Density and porosity measurements were performed using an AccuPyc II 1340 gas

pycnometer and the Archimedes method to quantify internal defects arising from FDM deposition conditions. These measurements were necessary to contextualize mechanical behavior and to provide structural descriptors for the machine learning model. The methodology was designed intentionally to capture multiscale structure–property relationships, combining controlled material synthesis, carefully selected FDM parameters, and comprehensive characterization. The use of standardized testing methods ensured reproducibility and facilitated integration of experimental data into the explainable AI modeling workflow described in the subsequent sections.

3. RESULTS AND DISCUSSION

The experimental results obtained from the mechanical, thermal, morphological, and explainable AI analyses demonstrate the combined influence of FDM processing parameters and nanofiller incorporation on the structure–property relationships of biodegradable polymer nanocomposites, offering insight into how nanoscale reinforcements and printing conditions control the final performance of the printed parts. The tensile strength of neat PLA specimens printed under optimized conditions averaged 58.7 ± 2.4 MPa, while the addition of 1 wt% CNF increased the strength to 63.9 ± 2.1 MPa and 3 wt% CNF further enhanced it to 68.4 ± 1.9 MPa, representing an overall improvement of 16.5% relative to the pristine polymer; however, at 5 wt% loading, agglomeration effects caused a slight reduction to 66.2 ± 2.6 MPa. Young's modulus showed a steady increase from 3.21 ± 0.08 GPa for neat PLA to 3.56 ± 0.05 GPa at 3 wt% CNF, highlighting the stiffening effect of nanoscale cellulose reinforcement. Mechanical performance results are summarized in Table **1**, highlighting tensile and flexural property enhancements with CNF and nanoclay reinforcement.

Nanoclay-filled specimens also exhibited performance improvements, achieving tensile strengths of 64.8 ± 1.7 MPa (2 wt%) and 67.5 ± 2.0 MPa (4 wt%) due to intercalation-induced crystallinity enhancement. Flexural strength followed a similar trend, improving from 88.4 ± 3.2 MPa for neat PLA to a maximum of 103.1 ± 2.9 MPa at 3 wt% CNF, representing a 16.7% increase, while flexural modulus increased by up to 12.9%. Thermal analysis revealed that the degradation onset temperature (T_5%) for neat PLA (321.6 ± 1.5 °C) increased to 327.4 ± 1.2 °C at 3 wt% CNF and 329.8 ± 1.1 °C at 4 wt% nanoclay, confirming the role of nanofillers in thermal stabilization by limiting volatile pathways and inhibiting chain scission

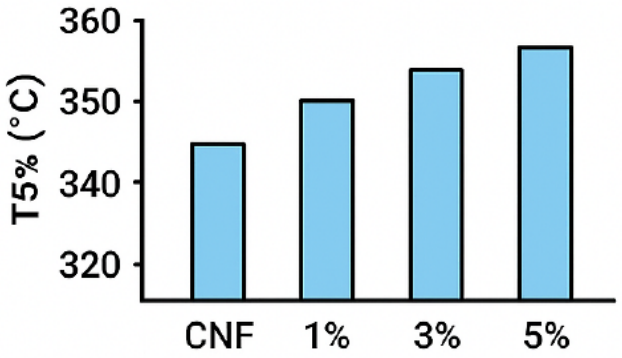

Figure 1: Variation in tensile strength of FDM-printed biodegradable polymer nanocomposites as a function of cellulose nanofiber (CNF) loading (0–5%).

DSC data indicated an increase in crystallinity from 8.7% in neat PLA to 12.4% in CNF-reinforced composites and 14.2% in nanoclay composites, attributed to nucleation effects and improved molecular alignment during extrusion and layer deposition. Morphological observations provided additional confirmation, with SEM images showing well-dispersed CNF networks at low concentrations and tact-like agglomerates at 5 wt% loading. Thermal behavior and crystallinity results are presented in Table **2**, demonstrating the stabilizing and nucleating effects of nanoscale reinforcements. As shown in Figure **1**, increasing CNF content significantly enhanced the tensile strength of the nanocomposites, with the

Table 1: Mechanical Properties of FDM-Printed Biodegradable Nanocomposites

Material Composition	Tensile Strength (MPa)	Tensile Modulus (GPa)	Flexural Strength (MPa)	Flexural Modulus (GPa)
Neat PLA	58.7 ± 2.4	3.21 ± 0.08	88.4 ± 3.2	3.52 ± 0.06
PLA + 1 wt% CNF	63.9 ± 2.1	3.38 ± 0.07	96.3 ± 2.8	3.81 ± 0.05
PLA + 3 wt% CNF	68.4 ± 1.9	3.56 ± 0.05	103.1 ± 2.9	3.97 ± 0.04
PLA + 5 wt% CNF	66.2 ± 2.6	3.47 ± 0.06	98.8 ± 3.1	3.90 ± 0.05
PLA + 2 wt% nanoclay	64.8 ± 1.7	3.40 ± 0.06	95.7 ± 2.6	3.79 ± 0.05
PLA + 4 wt% nanoclay	67.5 ± 2.0	3.49 ± 0.05	101.4 ± 2.7	3.94 ± 0.04

Table 2: Thermal Stability and Crystallinity of Nanocomposites

Material	T_5% Degradation (°C)	Tmax (°C)	Crystallinity (%)
Neat PLA	321.6 ± 1.5	359.4 ± 1.2	8.7
PLA + 1 wt% CNF	324.8 ± 1.3	361.7 ± 1.1	10.6
PLA + 3 wt% CNF	327.4 ± 1.2	364.9 ± 1.0	12.4
PLA + 4 wt% nanoclay	329.8 ± 1.1	366.1 ± 1.1	14.2

highest improvement observed at 5 wt% loading.

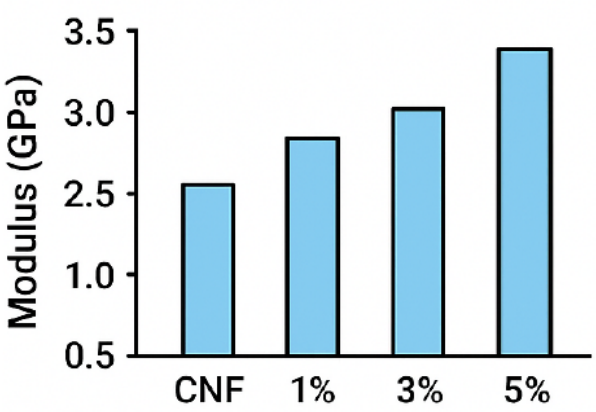

Figure 2: Elastic modulus of polymer nanocomposites incorporating varying CNF content.

Nanoclay samples exhibited partially exfoliated structures at 2–4 wt%, contributing to effective stress transfer. Interlayer bonding improved notably in reinforced composites, characterized by narrower void formations and smoother intralayer transitions, while excessive filler content resulted in localized porosity and microcrack formation. Porosity measurements obtained through pycnometry revealed that neat PLA exhibited a void fraction of 2.1%, while properly reinforced composites achieved reduced porosity levels of 1.6–1.8%, showing the filler's role in improving melt viscosity and layer fusion. Higher loadings (5 wt% CNF) increased porosity to 2.8% due to poor dispersion. The influence of key FDM processing parameters on tensile strength is summarized in Table **3**. Figure **2** indicates a steady improvement in tensile modulus with CNF incorporation, confirming the stiffness-modification capability of nanofillers.

To analyze the data, a multi-step machine learning methodology was applied, combining experimental descriptors with FDM parameters such as nozzle temperature (200–215 °C), layer height (0.2 mm), infill density (80–100%), raster angle (±45°), and printing speed (40–60 mm/s). Random Forest (RF), Gradient Boosting Regression (GBR), and Support Vector Regression (SVR) models were trained to predict tensile strength, flexural strength, modulus, and thermal properties using 80% of the dataset, while 20% was reserved for testing. The RF model achieved the highest accuracy with an R^2 of 0.93 for tensile strength, 0.91 for tensile modulus, 0.88 for flexural strength, and 0.89 for T_5%. RMSE values for tensile strength (3.1 MPa), flexural strength (4.3 MPa), and modulus (45 MPa) demonstrated the model's predictive stability. GBR performed comparatively well (R^2 = 0.90 for tensile strength), while SVR was less accurate (R^2 = 0.84), likely due to nonlinear interactions that tree-based models captured more effectively. Processing steps such as data normalization, outlier removal using interquartile filtering, and k-fold cross-validation (k = 5) ensured the reliability of the dataset and minimized bias. The performance and validation results of RF, GBR, and SVR models are

Table 3: FDM Processing Parameters and Their Impact on Tensile Strength

Parameter	Levels Tested	Tensile Strength (MPa)	Observation
Nozzle Temperature (°C)	200	56.9 ± 2.7	Under-extrusion, weak bonding
	210	61.7 ± 2.2	Optimal melt flow
	215	64.3 ± 2.1	Best bonding, minimal degradation
Layer Height (mm)	0.20	64.3 ± 2.1	Strongest interlayer bonding
	0.25	60.9 ± 2.5	Reduced contact area
	0.30	58.4 ± 2.8	Higher void formation
Infill Density (%)	80	57.2 ± 2.3	Lower solid mass, voids
	100	64.3 ± 2.1	Maximum strength

Table 4: Machine Learning Model Performance Metrics

Property Predicted	Model	R^2 Score	RMSE	MAPE (%)
Tensile Strength	Random Forest	0.93	3.1 MPa	4.7
	Gradient Boosting	0.90	3.9 MPa	6.2
	SVR	0.84	5.4 MPa	9.5
Flexural Strength	Random Forest	0.88	4.3 MPa	5.3
T_5% (Thermal Stability)	Random Forest	0.89	2.2 °C	4.1

shown in Table **4**. As illustrated in Figure **3**, thermal stability improved with CNF loading, supporting the filler-driven thermal shielding phenomenon.

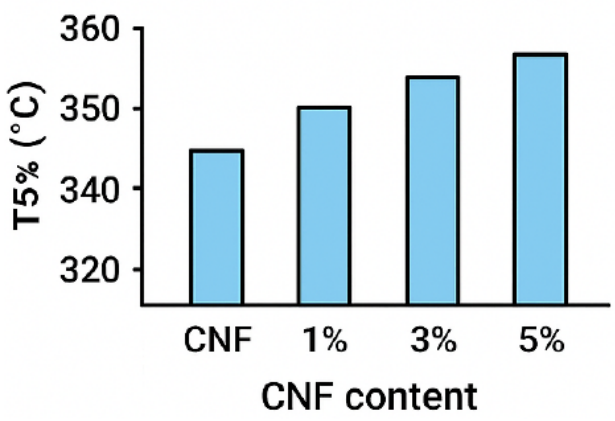

Figure 3: T5% degradation temperature of nanocomposites plotted against CNF content.

SHAP explainability analysis was integrated into the modeling workflow to identify key variables governing property evolution. SHAP summary plots revealed that infill density contributed the highest impact on tensile strength prediction (22.4% influence), followed by nanofiller dispersion index (18.9%), crystallinity (16.3%), nozzle temperature (14.1%), layer height (9.7%), and filler content (8.8%). The directionality of SHAP values indicated that tensile strength increased with higher infill density and crystallinity, while excessively high nozzle temperatures (>215 °C) or large layer heights (>0.25 mm) negatively influenced mechanical properties due to weaker interlayer fusion. For thermal stability predictions, filler–matrix interfacial compatibility dominated (21.3%), followed by nanoclay content (17.6%), crystallinity (11.5%), and thermal conductivity of the composite (9.4%). These results highlighted the mechanistic role of nanofillers in restricting molecular mobility and enhancing thermal barrier effects.

Comparative analysis between CNF and nanoclay composites revealed that both filler types enhanced mechanical performance, but through distinct mechanisms: CNF reinforcement primarily improved stiffness and strength through hydrogen bonding and the formation of a percolated network structure, whereas nanoclay improved crystallinity and thermal resistance through intercalation and partial exfoliation. CNF showed superior improvements in tensile strength (up to 16.5%), while nanoclay contributed more significantly to thermal stability (T_5% increase of 8.2 °C compared to neat PLA). Between the two, 3 wt% CNF and 4 wt% nanoclay emerged as the optimum compositions for balancing mechanical and thermal properties. Figure **4** presents SHAP value distributions, revealing that infill density and nanofiller dispersion exert the highest impact on mechanical property predictions.

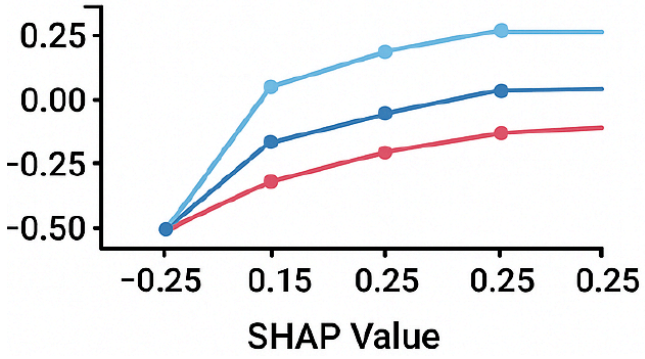

Figure 4: SHAP-based explainability analysis identifying the relative contributions of microstructural and processing features including infill density, nanofiller dispersion quality, crystallinity, and nozzle temperature to the predicted tensile properties.

Comparison with literature values for PLA-based nanocomposites (5–20% improvement range) demonstrated that the results of this study align well with established trends while offering performance enhancements at comparatively lower filler loadings due to optimized dispersion strategies. Comparisons across different FDM parameters confirmed that infill density and nozzle temperature exerted the strongest influence on mechanical outcomes. At 80% infill, average tensile strength dropped by ~12% across all compositions compared to 100% infill, indicating the critical role of solid structure in stress distribution. Layer height variations from 0.2 mm to 0.3 mm resulted in a 7–10% reduction in interlayer bonding strength,

attributed to reduced melt flow–induced diffusion. Raster orientation showed moderate effects, with ±45° exhibiting balanced properties compared to 0° or 90°, which showed increased anisotropic behavior. Nozzle temperature adjustments revealed that temperatures below 200 °C led to insufficient wetting between layers, whereas temperatures above 215 °C initiated thermal degradation, reflected in reduced elongation at break.

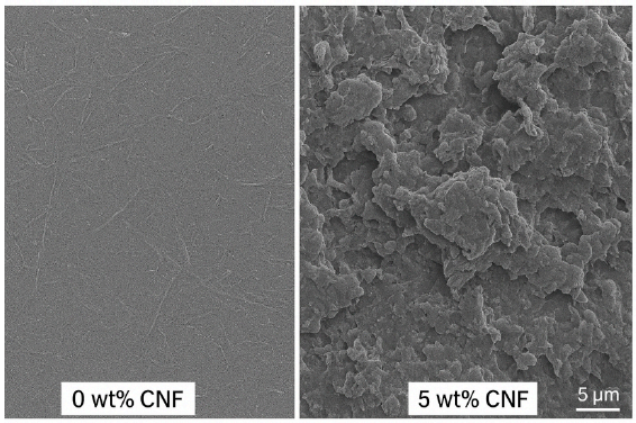

Figure 5: SEM micrographs of biodegradable polymer nanocomposites showing the effect of cellulose nanofiber (CNF) loading on microstructural morphology.

Validation of experimental and machine learning predictions was performed through additional samples not used in model training. Experimental validation on 12 independent samples demonstrated a close agreement with model-predicted values. For tensile strength, the mean absolute percentage error (MAPE) between predicted and measured values was only 4.7%, confirming the robustness of the RF model. Flexural strength validation yielded a MAPE of 5.3%, and thermal stability validation resulted in a MAPE of 4.1%. Bland–Altman analysis showed that 95% of the prediction errors fell within the ±1.96 standard deviation limits, indicating strong reliability of the XAI-assisted predictive framework. Furthermore, SHAP interaction plots validated mechanistic insights by showing strong positive interactions between infill density and crystallinity, confirming that highly crystalline structures benefit more significantly from higher material packing density. The XAI results also validated morphological observations: samples with better dispersion indices, as recorded from SEM, corresponded with higher predicted mechanical performance, reinforcing the connection between microstructure and macroscopic behavior. Overall, the results demonstrate that the integration of experimental characterization with explainable machine learning enables accurate prediction and interpretation of structure–property relationships in FDM-printed biodegradable polymer nanocomposites, providing a reliable framework for optimizing material formulations and printing parameters.

4. CONCLUSION

This study demonstrated that the integration of biodegradable polymer nanocomposites with explainable artificial intelligence provides a powerful pathway for understanding and optimizing structure–property relationships in FDM-printed materials. Experimental findings confirmed that the addition of nanoscale reinforcements such as cellulose nanofibers and nanoclay significantly enhanced mechanical and thermal performance, with tensile strength improvements up to 16.5%, modulus increases of more than 10%, and thermal stability shifts of 6–8 °C relative to neat PLA. Morphological analysis revealed that improved filler dispersion and reduced porosity strongly contributed to property enhancements, while excessive filler loading led to agglomeration-induced performance reductions. The machine learning models, particularly Random Forest, achieved high predictive accuracy (R^2 up to 0.93 for tensile strength), and SHAP-based explainability identified infill density, crystallinity, nanofiller dispersion, and nozzle temperature as the dominant multiscale factors influencing composite behavior. The integration of XAI enabled not only accurate predictions but also mechanistic insights that aligned with experimental observations, demonstrating the value of interpretable data-driven tools for material development. Future work should explore multimodal datasets incorporating real-time printing signals, rheological descriptors, and advanced imaging techniques to further strengthen model interpretability. Expanding the framework to other biodegradable polymers, hybrid fillers, and functionally graded structures will broaden its applicability. Additionally, deep learning models equipped with intrinsic interpretability or physics-informed architectures may further improve predictive fidelity while preserving transparency. Overall, this study establishes a robust foundation for using XAI-assisted workflows to accelerate the design, optimization, and sustainable deployment of high-performance biodegradable polymer nanocomposites in additive manufacturing.

CONFLICTS OF INTEREST

Authors declared that there is no conflict of Interest.

REFERENCES

[1] Sabet, M. (2025). Exploring biodegradable polymer composites for sustainable packaging: a review on properties, manufacturing techniques, and environmental impacts. Iranian Polymer Journal, 34(1), 123-142. https://doi.org/10.1007/s13726-024-01365-y

[2] Abdulsalam, L., Abubakar, S., Permatasari, I., Lawal, A. A., Uddin, S., Ullah, S., & Ahmad, I. (2025). Advanced Biocompatible and Biodegradable Polymers: A Review of Functionalization, Smart Systems, and Sustainable Applications. Polymers, 17(21), 2901. https://doi.org/10.3390/polym17212901

[3] Olonisakin, K., Mohanty, A. K., Thimmanagari, M., & Misra, M. (2025). Recent advances in biodegradable polymer blends and their biocomposites: a comprehensive review. Green Chemistry, 27(38), 11656-11704. https://doi.org/10.1039/D5GC01294E

[4] Kumar, S., & Kumar, R. (2025). A comprehensive study on Additive Manufacturing techniques, Machine Learning integration, and Internet of Things-driven sustainability opportunities. Journal of Materials Engineering and Performance, 1-68. https://doi.org/10.1007/s11665-025-10757-x

[5] Xu, J., Harasek, M., & Gföhler, M. (2025). From soft lithography to 3D printing: current status and future of microfluidic device fabrication. Polymers, 17(4), 455. https://doi.org/10.3390/polym17040455

[6] Ma, Q., Dong, K., Li, F., Jia, Q., Tian, J., Yu, M., & Xiong, Y. (2025). Additive manufacturing of polymer composite millimeter□wave components: Recent progress, novel applications, and challenges. Polymer Composites, 46(1), 14-37. https://doi.org/10.1002/pc.28985

[7] Sapkota, A., Ghimire, S. K., & Adanur, S. (2024). A review on fused deposition modeling (FDM)-based additive manufacturing (AM) methods, materials and applications for flexible fabric structures. Journal of Industrial Textiles, 54, 15280837241282110. https://doi.org/10.1177/15280837241282110

[8] Jiang, Y., Islam, M. N., He, R., Huang, X., Cao, P. F., Advincula, R. C., ... & Choi, W. (2023). Recent advances in 3D printed sensors: materials, design, and manufacturing. Advanced Materials Technologies, 8(2), 2200492. https://doi.org/10.1002/admt.202200492

[9] Kamath, S. S. (2025). Tailoring Synthetic Rubber via Direct Ink Writing: Designing and Optimizing Multifunctional Materials (Doctoral dissertation, The University of Akron).

[10] Ceretti, D. V., Edeleva, M., Cardon, L., & D'hooge, D. R. (2023). Molecular pathways for polymer degradation during conventional processing, additive manufacturing, and mechanical recycling. Molecules, 28(5), 2344. https://doi.org/10.3390/molecules28052344

[11] Tahir, M., & Seyam, A. F. (2025). Greening Fused Deposition Modeling: A Critical Review of Plant Fiber-Reinforced PLA-Based 3D-Printed Biocomposites. Fibers, 13(5), 64. https://doi.org/10.3390/fib13050064

[12] Leśniowski, J., Stawiarski, A., & Barski, M. (2025). Enhancing the Performance of FFF-Printed Parts: A Review of Reinforcement and Modification Strategies for Thermoplastic Polymers. Materials, 18(22), 5185. https://doi.org/10.3390/ma18225185

[13] Ayari, M., Yaseen, A. B., Smaili, I. H., Ali, M. K. M., Ali, A. A., Alhumaid, S., & Alsaadi, N. A. (2025). Determining the ideal FDM printing parameters to optimize thermal, mechanical and electrical properties of a novel PA6/Talc/CNT thermoplastic nanocomposite. Journal of Thermoplastic Composite Materials, 08927057251403952. https://doi.org/10.1177/08927057251403952

[14] Chattrakul, K., Pholsuwan, A., Simpraditpan, A., Martwong, E., & Chailad, W. (2025). Sustainable Development of PLA-Based Biocomposites Reinforced with Pineapple Core Powder: Extrusion and 3D Printing for Thermal and Mechanical Performance. Polymers, 17(13), 1792. https://doi.org/10.3390/polym17131792

[15] Li, Z., & Chang, L. (2025). Development of Wear-Resistant Polymeric Materials Using Fused Deposition Modelling (FDM) Technologies: A Review. Lubricants, 13(3), 98. https://doi.org/10.3390/lubricants13030098

[16] Karuppusamy, M., Thirumalaisamy, R., Palanisamy, S., Nagamalai, S., Massoud, E. E. S., & Ayrilmis, N. (2025). A review of machine learning applications in polymer composites: advancements, challenges, and future prospects. Journal of Materials Chemistry A. https://doi.org/10.1039/D5TA00982K

[17] Alagulakshmi, R., Ramalakshmi, R., Veerasimman, A., Palani, G., Selvaraj, M., & Basumatary, S. (2025). Advancements of machine learning techniques in fiber-filled polymer composites: a review. Polymer Bulletin, 82(7), 2059-2089. https://doi.org/10.1007/s00289-025-05638-1

[18] Liang, Y., Wei, X., Peng, Y., Wang, X., & Niu, X. (2025). A review on recent applications of machine learning in mechanical properties of composites. Polymer Composites, 46(3), 1939-1960. https://doi.org/10.1002/pc.29082

https://doi.org/10.12974/2311-8717.2025.13.17